

MicroRNA-124 regulates cell pyroptosis during cerebral ischemia-reperfusion injury by regulating STAT3

HUI SUN^{1,2}, JING-JING LI^{1,2}, ZI-REN FENG^{1,2}, HAI-YING LIU^{1,2} and AI-GUO MENG^{1,2}

¹Department of Clinical Laboratory; ²Key Laboratory of Medical Molecular Testing and Diagnosis, Affiliated Hospital of North China University of Science and Technology, Tangshan, Hebei 063000, P.R. China

Received December 1, 2019; Accepted July 1, 2020

DOI: 10.3892/etm.2020.9357

Abstract. Cerebral ischemia-reperfusion injury (CIRI) is the observed continuation and deterioration of ischemic injury, and currently, there are no effective treatment strategies for the condition. It has been reported that microRNAs (miRNAs) serve an important role in CIRI by regulating pyroptosis. The present study demonstrated that miRNA-124 regulated CIRI by regulating STAT3. To explore the relationship between miRNA-124/STAT3 and pyroptosis in CIRI, CIRI was simulated using a middle cerebral artery occlusion model. Subsequently, miRNA-124 expression levels were altered via the intracerebroventricular injection of miRNA-124 agonist or antagonist. The degree of brain tissue injury was assessed by conducting TTC staining and neurological function scoring. Relative miRNA-124 expression levels were determined via reverse transcription-quantitative PCR. A luciferase reporter gene system verified the targeted binding of miRNA-124 to STAT3. The expression levels of key proteins and proinflammatory cytokines associated with pyroptosis [caspase-1, gasdermin D, interleukin (IL)-18 and IL-1 β] were detected via western blotting and immunohistochemistry. The increased expression levels of pyroptosis-associated proteins and proinflammatory cytokines in the I/R groups compared with the control group, indicated that pyroptosis intensified over time during CIRI, and miRNA-124 agonist significantly abrogated pyroptosis and improved neurological function compared with the control group. Furthermore, miRNA-124 inhibited STAT3 activation in a targeted manner, which also decreased the extent of pyroptosis. However, miRNA-124 antagonist reversed miR-124 agonist-mediated effects. Therefore, the present study indicated that miRNA-124 may provide neuroprotection

against pyroptosis during CIRI, potentially via inhibition of the STAT3 signaling pathway.

Introduction

Epidemiological studies have revealed that ischemic cerebrovascular disease (ICD) is the second leading cause of mortality in humans worldwide, with a continually rising incidence rate (1,2). Currently, thrombolysis and bypass grafting are the two most commonly used therapeutic strategies for the treatment of ICD; however, they are often unsuccessful, resulting in a lack of effective treatment strategies for cerebral ischemia-reperfusion (I/R) injury (CIRI) (3). Therefore, understanding the specific mechanisms underlying reperfusion injury is of clinical importance. Numerous studies have demonstrated that inflammation is an important pathological factor contributing to CIRI (4–6). It has also been reported that a particular type of proinflammatory programmed cell death, pyroptosis, also serves an important role in the pathogenesis of I/R injury (7).

The main biological characteristics of pyroptosis are dependent on caspase-1 (8). Cookson and Brennan (9) were the first to propose the concept of pyroptosis, which has subsequently been reported to occur during I/R injury in numerous organs, with the levels of pyroptosis reflecting the degree of I/R to a certain extent (10–12). Therefore, the identification of novel therapeutic targets to inhibit pyroptosis may lead to novel therapeutic strategies for CIRI.

Almost all *in vivo* physiological and pathological processes, such as growth and development, proliferation, inflammation, tumorigenesis and neurodegenerative diseases, are subject to microRNA (miRNA/miR)-mediated target gene expression regulation (13–15). In particular, miRNA-124 is highly expressed in the central nervous system, with 100 times higher expression levels in the central nervous system compared with other tissues (16). The increased expression levels of miRNA-124 exert important neuroprotective effects; for example, during the early stages of ischemic stroke, miR-124 injection decreased both oxygen deprivation- and glucose deprivation-induced neuronal damage (17). In addition, Ponomarev *et al* (18) demonstrated that increased miRNA-124 expression levels prevented allergic cerebrospinal meningitis by opposing microglial activation. The aforementioned study suggested that the neuroprotective effects of miRNA-124 may

Correspondence to: Professor Ai-Guo Meng, Department of Clinical Laboratory, Affiliated Hospital of North China University of Science and Technology, 73 South Jianshe Road, Tangshan, Hebei 063000, P.R. China
E-mail: tangshan201501@sina.cn

Key words: cerebral ischemia-reperfusion injury, microRNA-124, pyroptosis, STAT3, caspase-1, gasdermin D, interleukin-1 β , interleukin-18

be closely linked to its effects on inflammation. Therefore, it was hypothesized that pyroptosis, as a proinflammatory form of programmed cell death, may be modulated by miRNA-124 during CIRI; however, the specific mechanisms by which this occurs are not completely understood.

The present study aimed to investigate miRNA-124 expression levels during the early stage of CIRI in a rat model, as well as the level of pyroptosis, which was determined by analyzing the expression levels of caspase-1, gasdermin D, interleukin (IL)-18 and IL-1 β . Furthermore, the effects of altered miRNA-124 expression on STAT3 activation and the degree of pyroptosis were also investigated. The results of the present study provided a basis for determining the possible early pathogenic mechanisms underlying CIRI and for the development of improved clinical strategies.

Materials and methods

Animal studies. Rats were purchased from Beijing Huafukang Biotechnology Co., Ltd. and housed at the Animal Experimental Center of North China University of Technology at 20 \pm 2°C with 55 \pm 5% humidity, 12-h light/dark cycles, and access to food and water *ad libitum*. All rats were acclimatized for a week with food and water before experimental manipulation. The present study was approved by the Animal Ethics Committee of North China University of Technology (approval no. LX201901).

Middle cerebral artery occlusion (MCAO) model preparation and experimental grouping. A total of 58 adult male Sprague-Dawley rats (age, 50-60 days; weight, 250-280 g) were randomly divided into four groups: i) Control; ii) sham operation, iii) I/R; and iv) drug treatment. The I/R group was further divided into four subgroups: 3, 6, 12 and 24 h post-reperfusion, for sample collection. The drug treatment group was further divided into three subgroups: i) I/R + negative control (NC); ii) I/R + miRNA-124 agonist (agomiRNA-124); iii) and I/R + miRNA-124 antagonist (antagomiRNA-124). Rats were used for the following experiments: 2-3-5 triphenyl tetrazolium chloride (TTC) staining (n=14; sham (n=4), NC (n=3), agomiRNA-124 (n=3) and antagomiRNA-124 groups (n=4)); 30 were used for western blotting and reverse transcription-quantitative PCR (RT-qPCR; n=30; sham (n=4), control (n=4), I/R (n=12) and drug (n=10) groups); and immunohistochemistry (n=14; sham (n=4) and drug (n=10) groups). Rats in the I/R and drug groups were subjected to CIRI, rats in the sham operation group underwent the same surgical operation but without an inserted suture and rats in the control group were not subjected to surgical operation. MCAO was performed in the left hemisphere to induce CIRI as previously described (19,20). Briefly, rats were anesthetized with an intraperitoneal injection of 2% sodium pentobarbital (30 mg/kg) (21). Subsequently, the common carotid artery (CCA) was separated from the nerves and tissue to gently expose the internal carotid artery (ICA) and the external carotid artery (ECA). The ECA was clipped and the ECA stump was stretched to align it with the ICA. A length of 3.0 cm plugging-up suture (cat. no. 3600AAA; Guangzhou Jialing Biological Technology Co., Ltd.) with its rounded tip was inserted to cut off the origin of the middle cerebral artery. Finally, the microvascular clip was removed

and the thread was fastened. The length of insertion was 18.5-19.5 mm from the CCA bifurcation. Following ischemia for 2 h, the monofilament was removed to induce CIRI.

Drug administration and neurological deficit scoring. At 2 days prior to MCAO establishment, rats received an intracerebroventricular injection of 20 nM miRNA-124 agonist (5 μ l; Guangzhou RiboBio Co., Ltd.), 20 nM miRNA-124 antagonist (5 μ l; Guangzhou RiboBio Co., Ltd.) or 20 nM miRNA-124 negative control (5 μ l; Guangzhou RiboBio Co., Ltd.) for 5 consecutive days. All experiments were performed under anesthetic and the lateral ventricle was located [coordinates from the bregma: Anterior-posterior (AP)=-0.8 mm, lateral (L)=-1.5 mm, ventral (V)=-4.8 mm] based on a stereotaxic atlas. Animals with hind limb paralysis or paresis following surgery were excluded from the study to rule out the effects of anesthetics and operative failures. Three rats died from operation (sham operation group excluded two rats in TTC staining and immunohistochemistry respectively; control group excluded one rat).

Neurological deficits were scored by one investigator after the rats awakened. The scores were evaluated using the 5-point scale described by Longa *et al* (19) as follows: 0, no neurological deficit; 1, failure to adequately extend the left forepaw; 2, circling to the left; 3, falling to the left; 4, depressed level of consciousness without spontaneous walking; and 5, death. Rats subjected to MCAO without detectable neurological deficits or death were removed from the following experiments to exclude the interference arising from operative failures (Three rats that died were excluded).

RT-qPCR. Total RNA was extracted from brain tissues using the Total RNA Purification kit (Suzhou GenePharma Co., Ltd.). Total RNA was reverse transcribed into cDNA using an miRNA RT primer and MMLV reverse transcriptase (contained in Hairpin-itTM miRNA RT-PCR Quantitative kit; cat. no. E22007; Suzhou GenePharma Co., Ltd.), at 25°C for 30 min, 42°C for 30 min and 85°C for 5 min, then stored at 4°C, according to the manufacturer's protocol. Subsequently, qPCR was performed using the QuantStudio 6 Flex Detection system (Thermo Fisher Scientific, Inc.) and a rno-miRNA-124 probe Hairpin-itTM miRNA and U6 snRNA Normalization RT-PCR Quantitation kit (cat. no. E22007; Suzhou Jima Gene Co., Ltd.), according to the manufacturer's protocol. The following primers were used for qPCR: miRNA-124 forward, 5'-TGTCTTAAGGCACGCGGT-3' and reverse, 5'-TATGGTTGTTCACGACTCCTTCAC-3'; and miRNA-124 probe, 5'-ATGCC+GTCT+GTATGGTTGGATAGGGA-3', U6 forward, 5'-CGCTTCGGCAGCACATATACTAA-3' and reverse, 5'-TATGGAACGCTTCACGAATTTGC-3'. The following thermocycling conditions were used for qPCR: Initial denaturation at 95°C for 3 min; followed by 40 cycles of 12 sec at 95°C and 40 sec at 62°C; the fluorescence signal was collected after 40 cycles. miRNA expression levels were quantified using the 2^{- $\Delta\Delta$ C_q} method and normalized to the internal reference gene U6 (22).

Western blotting. Total protein was extracted from fresh cerebral cortex in the ischemic penumbra. Total protein was quantified using a bicinchoninic acid assay kit

(cat. no. PT0001; Beijing Leagene Biotechnology Co., Ltd.). Proteins (30 $\mu\text{g}/\text{lane}$) were separated via a 10% SDS-PAGE, transferred onto PVDF membranes and blocked with 5% BSA for 1 h at room temperature. Subsequently, the membranes were incubated at 4°C overnight with the following primary antibodies: Anti-gasdermin D (1:500; cat. no. sc-393581; Santa Cruz Biotechnology, Inc.), anti-STAT3 (1:1,000; cat. no. 12640; Cell Signaling Technology, Inc.), phosphorylated (p)-STAT3 (1:1,000; cat. no. 52075; Cell Signaling Technology, Inc.), anti-pro-caspase-1 (1:1,000; cat. no. ab179515; Abcam), anti-caspase-1 p20 (1:1,000; 2225, Cell Signaling Technology, Inc.), anti-IL-1 β (1:1,000, cat. no. 12242; Cell Signaling Technology, Inc.), anti-IL-18 (1:1,000; cat. no. ab71495; Abcam) or anti- β -actin (1:2,000; cat. no. T0023; BIOS). Following primary incubation, the membranes were incubated with horseradish peroxidase-conjugated anti-rabbit or anti-mouse secondary antibodies (1:5,000; ZB2307, Zsbio Commerce Store) for 2 h at 37°C. The membranes were rinsed three times with TBS-0.1% Tween-20 for 10 min. Protein bands were visualized using EXPlus ECL reagent (Beijing Zoman Biotechnology Co., Ltd.) and the expression levels were quantified using ImageJ software (version 1.6.0; National Institutes of Health) with β -actin as the loading control.

TargetScan and Dual-luciferase reporter assay. The online target gene prediction software TargetScan (http://www.targetscan.org/vert_72/) was used to analyze the potential target genes of miRNA-124 and find the STAT3 is one of the target genes of miRNA-124. Dual-luciferase reporter plasmids containing the wild-type (WT) or mutant (MT) 3'-untranslated region (UTR) of STAT3 (pGL3-Promoter Vector, R0531, Promega Corporation) were constructed. PC12 cells (1 \times 10⁵ cells/ml; Chinese Academy of Sciences Cell Bank) were co-transfected with plasmids (2 μg) and miRNA-124 mimics (50 nM) or miRNA-124 negative control (50 nM) using TurboFect transfection reagent (R0531, Thermo Fisher Scientific). The following cell groups were generated: i) WT plasmid + miRNA-124 negative control group (WT-STAT3 + NC); ii) WT plasmid + miRNA-124 mimic group (WT-STAT3 + miRNA-124); iii) MT plasmid + miRNA-124 negative control group (MT-STAT3 + NC); and iv) MT plasmid + miRNA-124 mimic group (MT-STAT3 + miRNA-124). At 48 h post-transfection, a dual-luciferase reporter assay system kit (cat. no. E1910; Promega Corporation) was used to determine the relative luciferase activity. Relative luciferase activity=Firefly luciferase/Renilla luciferase.

Immunohistochemistry. Animals were anesthetized with an intraperitoneal injection of 2% sodium pentobarbital (30 mg/kg) and the ascending aorta was immediately perfused with 4% paraformaldehyde. Subsequently, the brain tissue was fixed in 4% paraformaldehyde for 24 h at 4°C and the infarct sections were embedded in paraffin and cut into 3 μm slices. Sections were blocked in 10% normal goat serum (cat. no. SP-9000; OriGene Technologies) for 2 h at room temperature and then incubated at 4°C overnight with the following primary antibodies: Anti-gasdermin D (1:50; cat. no. sc-81868; Santa Cruz Biotechnology, Inc.), anti-caspase-1 (1:100; 2225, Cell Signaling Technology, Inc.), anti-IL-1 β

(1:100; cat. no. 12242; Cell Signaling Technology, Inc.) and anti-IL-18 (1:100; cat. no. ab52914; Abcam). Following primary incubation, the sections were incubated with Cy3-conjugated and fluorescein isothiocyanate-conjugated secondary antibodies (1:50; cat. no. ZF-0311; OriGene Technologies) for 1 h at room temperature. Stained sections were visualized using a DP-80 fluorescence microscope (Olympus Corporation) in ten randomly selected fields of view and the positive cell rate was calculated as follows: (Positive cells/total cells) \times 100%.

TTC staining. Brain tissues were obtained following 12 h reperfusion and immediately stored at -20°C for 30 min. Frozen brain tissue was cut into five coronal 2-mm thick sections. The sections were placed in TTC staining solution (cat. no. DK003; Beijing Leagene Biotech Co., Ltd.) to incubation at 37°C for 30 min in the dark, and turned over at 15 min. TTC staining solution reacted with the dehydrogenase in the healthy brain tissue to stain the healthy brain tissue red. By contrast, decreased dehydrogenase activity in the ischemic brain tissue was indicated by a pale color, as the lack of dehydrogenase did not react with the TTC staining solution. Subsequently, TTC stained brain tissue sections were fixed in 4% paraformaldehyde at 4°C for 24 h. ImageJ software (version 1.6.0; National Institutes of Health) was used to calculate the infarct area, which was expressed as a percentage (%) of the infarct area. The ischemic area ratio (%)=(sum of white ischemic areas)/(sum of brain slice areas) \times 100%.

Statistical analysis. Statistical analyses were performed using GraphPad Prism software (version 5.0; GraphPad Software, Inc.). Data are presented as the mean \pm SD with at least three experimental repeats. Statistical differences among multiple groups were determined using one-way ANOVA followed by Tukey's post hoc test. $P < 0.05$ was considered to indicate a statistically significant difference.

Results

Dynamic expression levels of pyroptosis-associated proteins and proinflammatory cytokines following CIRI. The western blotting results indicated that the expression levels of caspase-1 (Fig. 1A) and IL-18 (Fig. 1D) were significantly increased in the I/R groups compared with the control group, reaching a peak at 24 h following CIRI ($P < 0.05$). In addition, the expression levels of gasdermin D (Fig. 1B) and IL-1 β (Fig. 1C) were significantly increased in the I/R groups compared with the control group, peaking at 12 h but decreasing by 24 h following CIRI ($P < 0.05$). There was no significant difference in expression levels of pyroptosis-associated proteins and proinflammatory cytokines observed between the sham operation and control groups ($P > 0.05$; Fig. 1).

Dynamic expression levels of miRNA-124 following CIRI. The RT-qPCR results revealed that there was no significant difference in miRNA-124 expression levels between the sham operation and control groups ($P > 0.05$). The expression levels of miRNA-124 in the I/R groups were significantly increased compared with the control group ($P < 0.05$). At 12 h following CIRI, the relative expression levels of miRNA-124 were ~ 7 times higher compared with the control group.

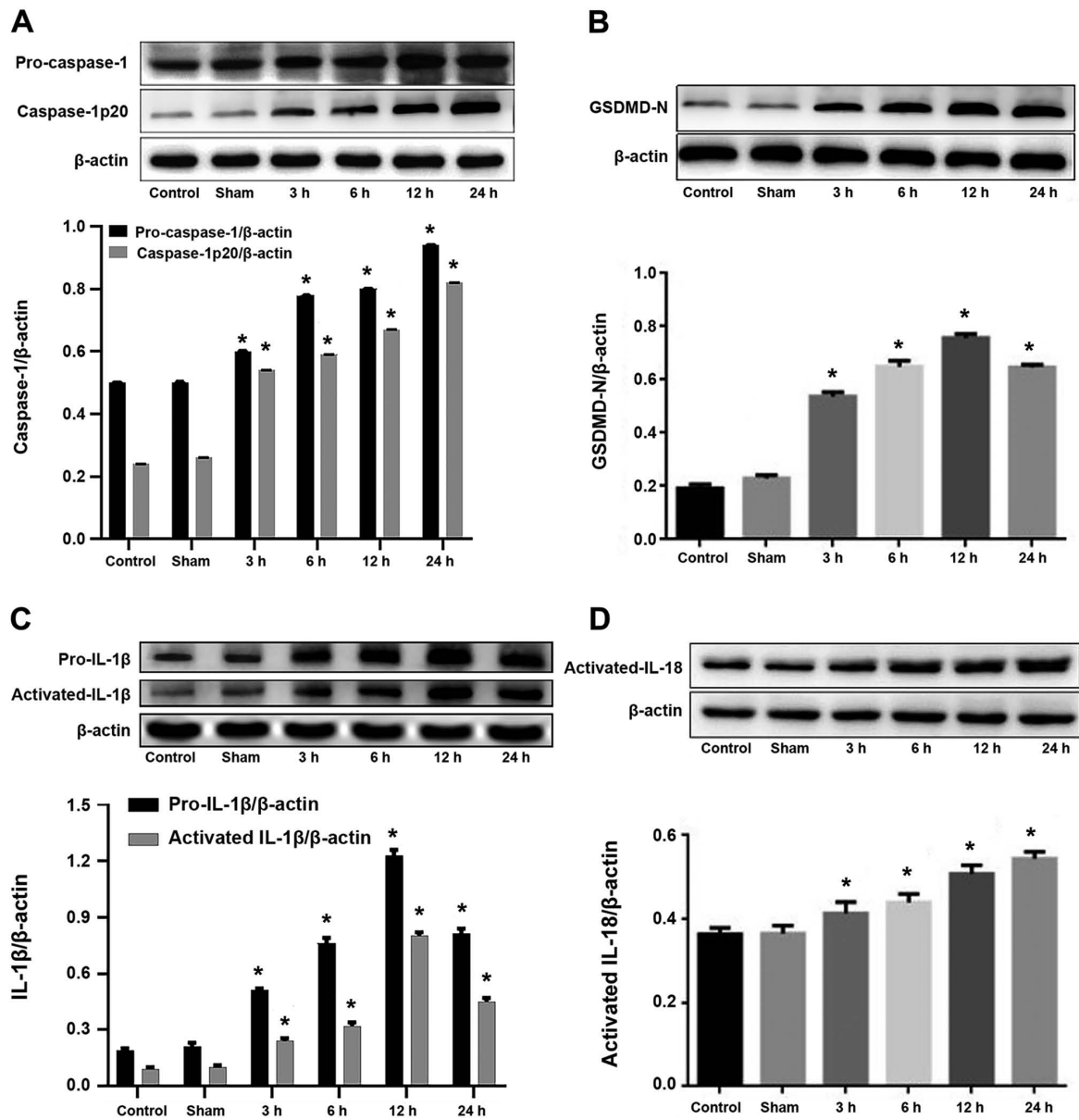


Figure 1. Expression levels of pyroptosis-associated proteins and proinflammatory cytokines following CIRI. Western blotting was performed to measure the protein expression levels of (A) caspase-1, (C) GSDMD-N, (C) IL-1β and (D) IL-18 in the negative control group, sham operation group, and ischemia-reperfusion group at 3, 6, 12 and 24 h following CIRI. * $P < 0.05$ vs. control. CIRI, cerebral ischemia-reperfusion injury; IL, interleukin; GSDMD, gasdermin D.

Between 12 and 24 h following CIRI, the expression levels of miRNA-124 decreased; however, the expression levels of miRNA-124 at 24 h were higher compared with the expression levels at 6 h (Fig. 2).

miR-124 serves a neuroprotective role in CIRI. The RT-qPCR results suggested that the expression levels of miR-124 in the NC group were significantly increased compared with the sham group ($P < 0.001$; Fig. 3A). Furthermore, the expression levels of miRNA-124 in the agomiRNA-124 and antagomiRNA-124 groups were significantly increased ($P < 0.05$; Fig. 3A) and decreased ($P < 0.001$; Fig. 3A) compared with the NC group, respectively, which indicated that the drugs were effective. The neurological function scores revealed that there was no obvious neurological deficit in the sham group. The neurological function score of the agomiRNA-124 group was significantly decreased compared with the NC group

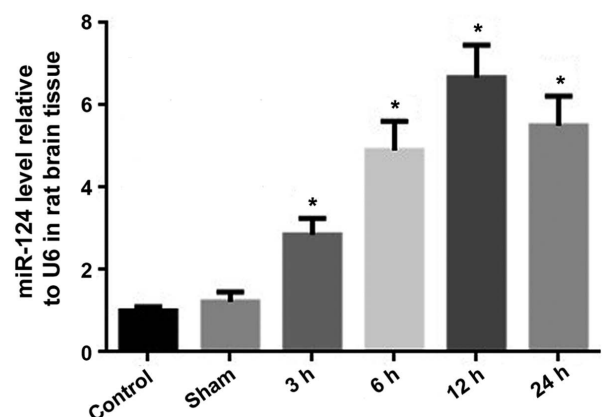


Figure 2. Relative miRNA-124 expression levels in the negative control group, sham operation group, and I/R group at 3, 6, 12 and 24 h following cerebral ischemia-reperfusion injury. * $P < 0.05$ vs. control. miRNA, microRNA; I/R, ischemia-reperfusion.

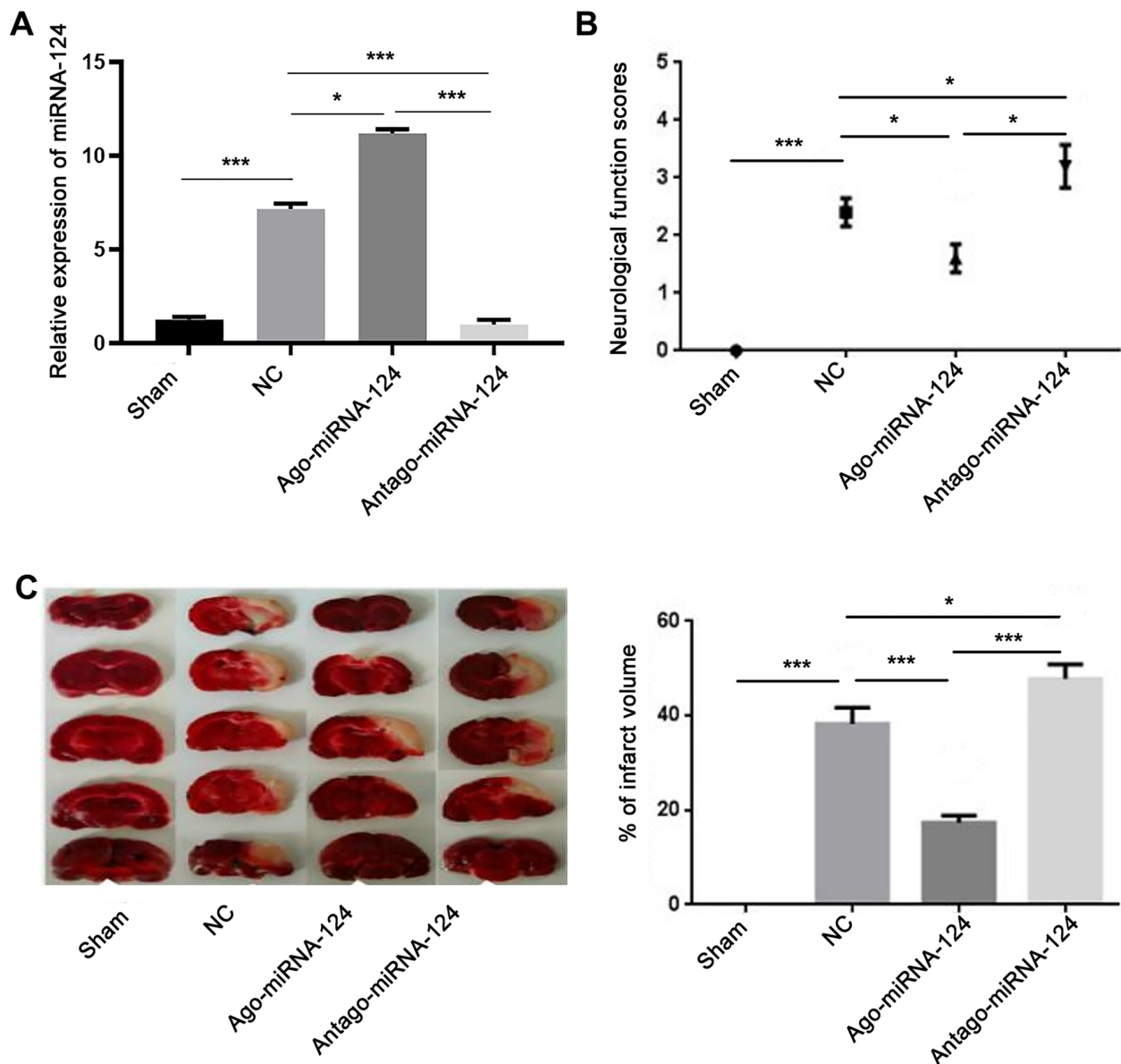


Figure 3. miR-124 serves a neuroprotective role in cerebral ischemia-reperfusion injury. (A) The relative expression of miRNA-124 in the sham, NC, agomiRNA-124 and antagomiRNA-124 groups. (B) The neurological function scores of the sham, NC, agomiRNA-124 and antagomiRNA-124 groups. (C) TTC staining of the sham, NC, agomiRNA-124 and antagomiRNA-124 groups. * $P<0.05$; *** $P<0.001$. miR, microRNA; NC, negative control.

($P<0.05$; Fig. 3B), whereas the neurological function score of the antagomiRNA-124 group was significantly increased compared with the NC and agomiRNA-124 groups ($P<0.05$; Fig. 3B). TTC staining also indicated that the infarct size in the agomiRNA-124 group was significantly decreased compared with the NC group ($P<0.001$; Fig. 3C), whereas the infarct size in the antagomiRNA-124 group was significantly increased compared with the NC group ($P<0.05$; Fig. 3B). The results suggested that increased expression levels of miRNA-124 may significantly reduce CIRI.

miR-124 inhibits STAT3 activation. TargetScan software identified a complementary binding site between miRNA-124 and the 3'-UTR of STAT3 (Fig. 4A). Subsequently, the dual-luciferase reporter assay demonstrated that the 3'-UTR of STAT3 bound to miRNA-124. Compared with the WT-STAT3 + NC group, the WT-STAT3 + miRNA-124 group displayed significantly reduced

relative luciferase activity ($P<0.05$; Fig. 4B). The western blotting results also suggested that the expression levels of STAT3 and p-STAT3 were significantly decreased in the agomiRNA-124 group compared with the NC group ($P<0.05$; Fig. 4C).

miRNA-124 inhibits pyroptosis in CIRI. Immunohistochemical staining was conducted to investigate the role of important proteins and proinflammatory cytokines involved in pyroptosis. No positive cells were observed in the sham operation group (Fig. 5), whereas the number of caspase-1- ($P<0.05$; Fig. 5A), gasdermin D- ($P<0.05$; Fig. 5B), IL-1 β - ($P<0.05$; Fig. 5C) and IL-18-positive cells ($P<0.05$; Fig. 5D) were significantly increased in the NC group compared with the sham operation group. miRNA-124 agonist significantly decreased the expression levels of caspase-1, gasdermin D, IL-1 β and IL-18 compared with the NC group, whereas antagomiRNA-124 displayed the opposite effect ($P<0.05$; Fig. 5E).

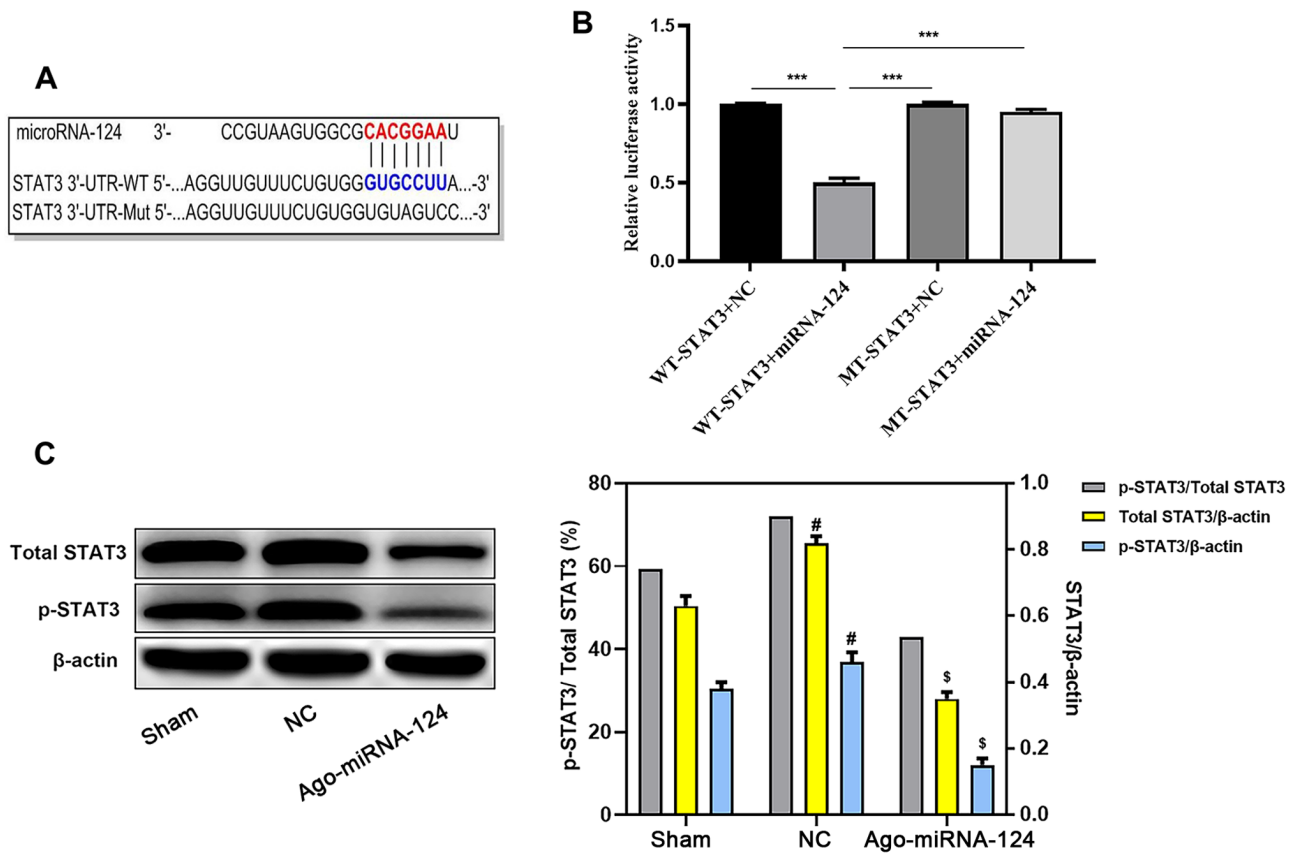


Figure 4. miR-124 inhibits STAT3 activation. (A) TargetScan software identified the complementary gene sequences between miRNA-124 and the 3'-UTR of STAT3. (B) The dual-luciferase reporter assay detected relative luciferase activities. (C) Western blotting was performed to measure the relative expression levels of p-STAT3 and total STAT3 in the sham, NC and agomiRNA-124 groups. ^{*}P<0.05 vs. NC, [#]P<0.05 vs. sham, ^{***}P<0.001. miR, microRNA; 3'UTR, 3'-untranslated region; p, phosphorylated; NC, negative control; WT, wild-type; Mut, mutant.

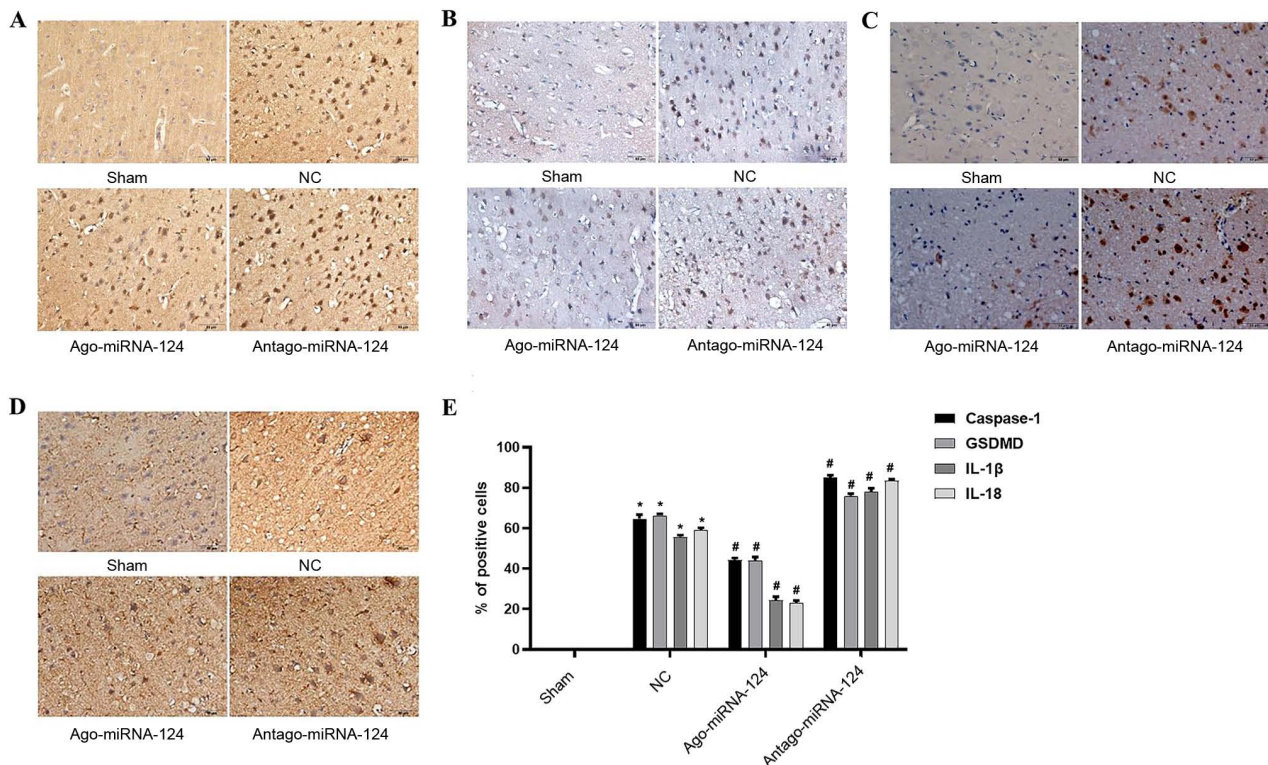


Figure 5. miRNA-124 inhibits pyroptosis in cerebral ischemia-reperfusion injury. Immunohistochemical staining was performed to investigate the expression of (A) caspase-1, (B) GSDMD, (C) IL-1β and (D) IL-18 in the sham, NC, agomiRNA-124 and antagomiRNA-124 groups (magnification, x400). (E) Quantification of immunohistochemical staining. ^{*}P<0.05 vs. NC; [#]P<0.05 vs. sham. IL, interleukin; NC, negative control; GSDMD, gasdermin D.

Discussion

CIRI is a major cause of death and disability in adults worldwide (23). Previous studies have reported the occurrence of apoptosis (24) and necroptosis (25) in CIRI, and that inhibition of caspase-1, an important mediator protein of pyroptosis, significantly reduced CIRI (26,27). Caspase-1 normally exists in the cytoplasm in the form of an inactive proenzyme, pro-caspase-1. Upon receiving danger signals, cells assemble into inflammatory bodies and recruit pro-caspase-1, resulting in a relatively high local concentration of pro-caspase-1. Subsequently, the autologous hydrolysis of the zymogen produces the activated form of caspase-1, caspase-1 p20, which then activates IL-1 β and IL-18 (28,29). Concurrently, activated caspase-1 has also been found to cleave gasdermin D, releasing the active N-terminal residue fragment, which binds to the cell membrane and forms a 10-15 nm pore. Collectively, the aforementioned events lead to the osmotic death of neurons and the release of intracellular mature proinflammatory cytokines (30). IL-1 β and IL-18 belong to the IL superfamily; both cytokines activate multiple inflammatory signaling pathways, resulting in the release of inflammatory cytokines. Activation of the inflammatory cascade can lead to the production of increased endogenous danger signals and can induce periphery pyroptosis (31). In the present study, the expression levels of caspase-1, caspase-1, gasdermin D, IL-1 β and IL-18 in the brain tissue were significantly increased following CIRI and following aggravation of CIRI compared with the control group. The results suggested that pyroptosis may be an important factor that aggravates CIRI, thus inhibiting pyroptosis may serve as an effective treatment strategy for CIRI.

It was recently discovered that the regulation of pyroptosis in I/R injury was mediated by miRNAs (32-34). miRNAs can affect pyroptosis by directly or indirectly regulating the expression of caspase-1. For example, miRNA-133 improves myocardial I/R injury by regulating the assembly of inflammatory bodies, inhibiting the activation of caspase-1 and reducing pyroptosis (32,33). miRNA-124 is a highly specific miRNA expressed in the central nervous system, which was observed to serve neuroprotective roles in a variety of nervous system diseases, such as ischemic stroke (17) and CIRI (34). The present study indicated that the expression levels of miRNA-124 increased following CIRI compared with the control group; however, the compensatory effect was weakened following aggravation of CIRI. In addition, an exogenous miRNA-124 injection significantly reduced the neuronal damage observed in the I/R group and significantly decreased the expression levels of pyroptosis-related proteins compared with the NC group. miRNA-124-induced effects were reversed by inhibiting the expression levels of miRNA-124, suggesting that miRNA-124 may serve a neuroprotective role in CIRI by inhibiting pyroptosis.

STAT3, an important member of the STAT family, is responsible for transmitting signals from activated plasma membrane receptors to the nucleus (35). Previous studies have reported that STAT3 affected the activation of caspase-1 by regulating the expression levels of inflammatory corpuscles (36,37). Previous bioinformatics analysis discovered that miRNA-124 targeted STAT3 (38). Therefore, it was hypothesized that

miRNA-124 may affect the degree of pyroptosis by regulating STAT3. The findings obtained in the present study further supported the hypothesis. The dual-luciferase reporter assay revealed that miRNA-124 bound to STAT3, and the experimental results and analysis demonstrated that the expression levels of STAT3 and p-STAT3 were decreased. Furthermore, the expression levels of caspase-1, gasdermin D, IL-1 β and IL-18 were decreased in the agomiRNA-124 group compared with the NC group. The results indicated that miRNA-124 may prevent the phosphorylation and subsequent activation of STAT3 into p-STAT3, thereby blocking pyroptosis and reducing neuronal damage following CIRI.

Previous studies have also revealed that miRNA-124 regulated neuronal injury following CIRI (14,18), with one study reporting that miRNA124 regulated proliferation and apoptosis via STAT3 (39). However, whether miR-124 regulates pyroptosis via STAT3 is not completely understood. The results of the present study revealed a potential mechanism underlying miRNA-124-mediated regulation of pyroptosis in CIRI, which may provide a novel therapeutic target. In view of the various injury mechanisms in CIRI, the present study indicated that miRNA-125 may serve a neuroprotective role in CIRI, but cannot completely cure the condition. Therefore, a strategy to cure CIRI required further investigation.

Acknowledgements

Not applicable.

Funding

No funding was received.

Availability of data and materials

The datasets used and/or analyzed during the present study are available from the corresponding author on reasonable request.

Authors' contributions

HS performed the immunohistochemistry, TTC staining and reverse transcription-quantitative PCR experiments as well as modified the manuscript. JL constructed the middle cerebral artery occlusion model, performed the western blotting experiments and analyzed the data. ZF and HL constructed the luciferase reporter plasmid technology, administered drugs and conducted neurological deficit scoring. AM designed the study and drafted the manuscript. All authors read and approved the final manuscript.

Ethics approval and consent to participate

The present study was approved by the Animal Ethics Committee of North China University of Technology (Tangshan, China; approval no. LX201901).

Patient consent for publication

Not applicable.

Competing interests

The authors declare that they have no competing interests.

References

- Murray CJ and Lopez AD: Measuring the global burden of disease. *N Engl J Med* 369: 448-457, 2013.
- Ahmad M, Dar NJ, Bhat ZS, Hussain A, Shah A, Liu H and Graham SH: Inflammation in ischemic stroke: Mechanisms, consequences and possible drug targets. *CNS Neurol Disord Drug Targets* 13: 1378-1396, 2014.
- Neuhaus AA, Couch Y, Hadley G and Buchan AM: Neuroprotection in stroke: The importance of collaboration and reproducibility. *Brain* 140: 2079-2092, 2017.
- Huang J, Wang T, Yu D, Fang X, Fan H, Liu Q, Yi G, Yi X and Liu Q: l-Homocarnosine attenuates inflammation in cerebral ischemia-reperfusion injury through inhibition of nod-like receptor protein 3 inflammasome. *Int J Biol Macromol* 118: 357-364, 2018.
- Han M, Hu L and Chen Y: Rutaecarpine may improve neuronal injury, inhibits apoptosis, inflammation and oxidative stress by regulating the expression of ERK1/2 and Nrf2/HO-1 pathway in rats with cerebral ischemia-reperfusion injury. *Drug Des Devel Ther* 13: 2923-2931, 2019.
- Liu Q and Zhang Y: PRDX1 enhances cerebral ischemia-reperfusion injury through activation of TLR4-regulated inflammation and apoptosis. *Biochem Biophys Res Commun* 519: 453-461, 2019.
- Li Z, Zhao F, Cao Y, Zhang J, Shi P, Sun X, Zhang F and Tong L: DHA attenuates hepatic ischemia reperfusion injury by inhibiting pyroptosis and activating PI3K/Akt pathway. *Eur J Pharmacol* 835: 1-10, 2018.
- Sborgi L, Ruhl S, Mulvihill E, Pipercevic J, Heilig R, Stahlberg H, Farady CJ, Muller DJ, Broz P and Hiller S: GSDMD membrane pore formation constitutes the mechanism of pyroptotic cell death. *EMBO J* 35: 1766-1778, 2016.
- Cookson BT and Brennan MA: Pro-inflammatory programmed cell death. *Trends Microbiol* 9: 113-114, 2001.
- Yang JR, Yao FH, Zhang JG, Ji ZY, Li KL, Zhan J, Tong YN, Lin LR and He YN: Ischemia-reperfusion induces renal tubule pyroptosis via the CHOP-caspase-11 pathway. *Am J Physiol Renal Physiol* 306: F75-F84, 2014.
- Kawaguchi M, Takahashi M, Hata T, Kashima Y, Usui F, Morimoto H, Izawa A, Takahashi Y, Masumoto J, Koyama J, *et al*: Inflammasome activation of cardiac fibroblasts is essential for myocardial ischemia/reperfusion injury. *Circulation* 123: 594-604, 2011.
- Zhu P, Duan L, Chen J, Xiong A, Xu Q, Zhang H, Zheng F, Tan Z, Gong F and Fang M: Gene silencing of NALP3 protects against liver ischemia-reperfusion injury in mice. *Hum Gene Ther* 22: 853-864, 2011.
- Ponomarev ED, Veremeyko T and Weiner HL: MicroRNAs are universal regulators of differentiation, activation, and polarization of microglia and macrophages in normal and diseased CNS. *Glia* 61: 91-103, 2013.
- Chang KP, Lee HC, Huang SH, Lee SS, Lai CS and Lin SD: MicroRNA signatures in ischemia-reperfusion injury. *Ann Plast Surg* 69: 668-671, 2012.
- Ge Y, Yan X, Jin Y, Yang X, Yu X, Zhou L, Han S, Yuan Q and Yang M: MiRNA-192 [corrected] and miRNA-204 directly suppress lncRNA HOTTIP and interrupt GLS1-mediated glutaminolysis in hepatocellular carcinoma. *PLoS Genet* 11: e1005726, 2015.
- Kynast KL, Russe OQ, Moser CV, Geisslinger G and Niederberger E: Modulation of central nervous system-specific microRNA-124a alters the inflammatory response in the formalin test in mice. *Pain* 154: 368-376, 2013.
- Taj SH, Kho W, Riou A, Wiedermann D and Hoehn M: MiRNA-124 induces neuroprotection and functional improvement after focal cerebral ischemia. *Biomaterials* 91: 151-165, 2016.
- Ponomarev ED, Veremeyko T, Barteneva N, Krichevsky AM and Weiner HL: MicroRNA-124 promotes microglia quiescence and suppresses EAE by deactivating macrophages via the C/EBP- α -PU.1 pathway. *Nat Med* 17: 64-70, 2011.
- Longa EZ, Weinstein PR, Carlson S and Cummins R: Reversible middle cerebral artery occlusion without craniectomy in rats. *Stroke* 20: 84-91, 1989.
- Yu ZH, Cai M, Xiang J, Zhang ZN, Zhang JS, Song XL, Zhang W, Bao J, Li WW and Cai DF: PI3K/Akt pathway contributes to neuro-protective effect of Tongxinluo against focal cerebral ischemia and reperfusion injury in rats. *J Ethnopharmacol* 181: 8-19, 2016.
- Song X, Zhou B, Zhang P, Lei D, Wang Y, Yao G, Hayashi T, Xia M, Tashiro S, Onodera S and Ikejima T: Protective effect of silibinin on learning and memory impairment in LPS-treated rats via ROS-BDNF-TrkB pathway. *Neurochem Res* 41: 1662-1672, 2016.
- Livak KJ and Schmittgen TD: Analysis of relative gene expression data using real-time quantitative PCR and the 2(-Delta Delta C(T)) method. *Methods* 25: 402-408, 2001.
- Ramos E, Patiño P, Reiter RJ, Gil-Martín E, Marco-Contelles J, Parada E, Rios C, Romero A and Egea J: Ischemic brain injury: New insights on the protective role of melatonin. *Free Radic Biol Med* 104: 32-53, 2017.
- Li PF, Shen MH, Gao F, Wu JP, Zhang JH, Teng FM and Zhang CB: An Antagomir to MicroRNA-106b-5p ameliorates cerebral ischemia and reperfusion injury in rats via inhibiting apoptosis and oxidative stress. *Mol Neurobiol* 54: 2901-2921, 2017.
- Nikseresht S, Khodagholi F and Ahmadiani A: Protective effects of ex-527 on cerebral ischemia-reperfusion injury through necroptosis signaling pathway attenuation. *J Cell Physiol* 234: 1816-1826, 2019.
- Fann DY, Lee SY, Manzanero S, Tang SC, Gelderblom M, Chunduri P, Bernreuther C, Glatzel M, Cheng YL, Thundiyil J, *et al*: Intravenous immunoglobulin suppresses NLRP1 and NLRP3 inflammasome-mediated neuronal death in ischemic stroke. *Cell Death Dis* 4: e790, 2013.
- Fann DY, Santoro T, Manzanero S, Widiapradja A, Cheng YL, Lee SY, Chunduri P, Jo DG, Stranahan AM, Mattson MP and Arumugam TV: Intermittent fasting attenuates inflammasome activity in ischemic stroke. *Exp Neurol* 257: 114-119, 2014.
- Lu A and Wu H: Structural mechanisms of inflammasome assembly. *FEBS J* 282: 435-444, 2015.
- Liu X and Lieberman J: A mechanistic understanding of pyroptosis: The fiery death triggered by invasive infection. *Adv Immunol* 135: 81-117, 2017.
- Shi J, Zhao Y, Wang K, Shi X, Wang Y, Huang H, Zhuang Y, Cai T, Wang F and Shao F: Cleavage of GSDMD by inflammatory caspases determines pyroptotic cell death. *Nature* 526: 660-665, 2015.
- Wei R, Wang J, Xu Y, Yin B, He F, Du Y, Peng G and Luo B: Probenecid protects against cerebral ischemia/reperfusion injury by inhibiting lysosomal and inflammatory damage in rats. *Neurosci* 301: 168-177, 2015.
- Xiao L, Jiang L, Hu Q and Li Y: MicroRNA-133b ameliorates allergic inflammation and symptom in murine model of allergic rhinitis by targeting Nlrp3. *Cell Physiol Biochem* 42: 901-912, 2017.
- Yu SY, Dong B, Tang L and Zhou SH: LncRNA MALAT1 sponges miR-133 to promote NLRP3 inflammasome expression in ischemia-reperfusion injured heart. *Int J Cardiol* 254: 50, 2017.
- Yang Q, Shi Q and Fu J: Applications of cerebrospinal miRNA in the detection and treatment of acute CNS injury. *Front Lab Med* 2: 83-88, 2018.
- Ray JP, Marshall HD, Laidlaw BJ, Staron MM, Kaech SM and Craft J: Transcription factor STAT3 and type I interferons are co-repressive insulators for differentiation of follicular helper and T helper 1 cells. *Immunity* 40: 367-377, 2014.
- Liu CC, Huang ZX, Li X, Shen KF, Liu M, Ouyang HD, Zhang SB, Ruan YT, Zhang XL, Wu SL, *et al*: Upregulation of NLRP3 via STAT3-dependent histone acetylation contributes to painful neuropathy induced by bortezomib. *Exp Neurol* 302: 104-111, 2018.
- Cuesta N, Nhu QM, Zudaire E, Polumuri S, Cuttitta F and Vogel SN: IFN regulatory factor-2 regulates macrophage apoptosis through a STAT1/3- and caspase-1-dependent mechanism. *J Immunol* 178: 3602-3611, 2007.
- Wei J, Wang F, Kong LY, Xu S, Doucette T, Ferguson SD, Yang YH, McEnery K, Jethwa K, Gjyshi O, *et al*: miR-124 inhibits STAT3 signaling to enhance T cell-mediated immune clearance of glioma. *Cancer Res* 73: 3913-3926, 2013.
- Nagata K, Hama I, Kiryu-Seo S and Kiyama H: microRNA-124 is down regulated in nerve-injured motor neurons and it potentially targets mRNAs for KLF6 and STAT3. *Neurosci* 256: 426-432, 2013.



This work is licensed under a Creative Commons Attribution-NonCommercial-NoDerivatives 4.0 International (CC BY-NC-ND 4.0) License.